Thin-Walled Structures 47 (2009) 1331–1342

Contents lists available at ScienceDirect

Thin-Walled Structures

journal homepage: www.elsevier.com/locate/tws

Y-stiffened panel multi-objective optimization using genetic algorithm

Sherif Farouk Badran [a,*], Ashraf O. Nassef [b], Sayed M. Metwalli [c]

[a] Marine Engineering Technology Department, Arab Academy for Science & Technology and Maritime Transportation. P.O. Box 1029, Abu Qir, Alexandria 21937, Egypt
[b] Mechanical Design and Production Department, Faculty of Engineering, American University in Cairo, 113 Kasr El Aini St., P.O. Box 2511, Cairo 11511, Egypt
[c] Mechanical Design and Production Department, Faculty of Engineering, Cairo University, Giza 12316, Egypt

ARTICLE INFO

Article history:
Received 3 August 2008
Received in revised form
13 March 2009
Accepted 13 March 2009
Available online 9 May 2009

Keywords:
Buckling
Y-stiffened panel
Genetic algorithm
Multi-objective functions

ABSTRACT

The aim of this paper is to design an optimum Y-stiffener plate combination using multi-objective optimization with real-coded genetic algorithms under the action of uniaxial compressive loads, because the most important loads applied on stiffened plates in ship hull is longitudinal in-plane axial compression arising for instance due to longitudinal bending because the cargo is not distributed equally in holds or due to grounding, stranding or collision. Five of the Y-stiffened panel dimensions were selected to be the independent design variables of the optimization problem. The objective functions are the ultimate buckling load and the volume per unit area of the Y-stiffener plate combination. Nonlinear finite element analysis was used to calculate the ultimate buckling load of 3^5 different sets of the design variables, with certain range for each of the design variables. The effects of independent design variables on the ultimate buckling load and the volume per unit area for Y-stiffener plate combination were studied and discussed. A new surrogate function to predict the ultimate buckling load of Y-stiffener plate combination is created and validated using the values of the ultimate buckling loads calculated using nonlinear finite element analysis. The proposed surrogate function is valid only in the specific ranges of the design variables. The Pareto optimal sets were calculated using multi-objective optimization with real-coded genetic algorithms and the optimum set of the independent design variables which is associated with the optimal geometric dimensions of the Y-stiffened panel was selected as the set which has the maximum ultimate buckling load to volume per unit area ratio. The optimum set was tested and validated using sensitivity analysis technique.

1. Introduction

Longitudinal in-plane axial compression is the most important loads applied on stiffened plates in ship hull, so the designers to aspire improved constructions that are capable of withstanding the longitudinal in-plane axial compression that produces from different loads. These improved structures can as well lead to commercial profit, since it allows increased cargo loads at a decreased risk level. The design of hull girders considers the hull girder as a system consisting of three subsystems; deck, side and bottom substructures. Each of these substructures can be divided into panels consisting of stiffening elements with their attached plating. Such panels are assumed to be supported by transverse frames, and are the basic elements of all types of ship structures. There are many computational, mathematical and numerical methods by using optimization techniques which are used to know the behavior of structures under impact load caused by collisions and groundings or stranding. This paper is concerned with the structural optimization of the buckling load of Y-stiffened panel.

Many researchers such as Timoshenko and Gere [1], Bleich [2] and Paik and Thayamballi [3] have contributed to ship plating using conventional stiffeners such as tee, angle and flat stiffeners. T-stiffener has been studied, and the elastic buckling coefficient has been calculated under suitable boundary conditions by Paik et al. [4]. Y-stiffener is discussed by Ludolphy [5]. Badran et al. (2007) studied the stability of Y-stiffener by calculating the elastic buckling coefficient of the weakest part of Y-stiffener and calculated the critical buckling stress and buckling load of Y-stiffener and using curve fitting of the analytically obtained results, approximate expressions for calculation of the elastic buckling coefficients of the T-part of the Y-stiffener are obtained [6]. Badran et al. (2008) studied the stability of Y-stiffener and equivalent T-stiffener under suitable two groups of boundary conditions, and the obtained results showed that the critical buckling loads for Y-stiffener is larger than that for equivalent T-stiffener by 41% for the first group of boundary conditions. The second group showed that the Y-stiffener plate combination is five times larger than the equivalent T-stiffener [7]. A qualitative assessment of 10 different steel sandwich alternatives to identify potential novel crashworthy side shell structures has been made

* Corresponding author. Tel.: +20 3 5564575; fax: +20 1 530 884 5041.
E-mail address: Sherif_badran@yahoo.com (S.F. Badran).

0263-8231/$ - see front matter © 2009 Elsevier Ltd. All rights reserved.
doi:10.1016/j.tws.2009.03.011

by Klanac, Ehlers et al. [8] and the results are compared with the performance of a conventional double side. One variant of a novel structure offered 40% higher capacity to absorb collision energy. K. Ghavami and R.M. Reza Khedmati presented the results of the finite element method (FEM) for nonlinear analysis of conventional stiffened plates subjected to axial compression load considering post-buckling behavior up to collapse [9]. The bifurcation analysis of thin-walled members subjected to uniform compression using an elastic nonlinear finite strip buckling method to determine the flexural and torsional tangent rigidities of a channel columns, undergoing local buckling, has been presented by Ben [10]. The calculation of the load carrying capacity of composite structures as well as to present comparison of the calculations obtained with the finite element method and the approximate method based on the linear analysis of critical loads are presented by Kolakowski and Kubiak [11]. Yong has studied buckling and collapse of columns and beam columns. He studied the ultimate strength of plates and stiffened plates and collapse analysis of ship hulls and used the nonlinear finite element in some calculations [12].

The loads acting on a stiffened panel in a ship are in-plane compression or tension, resulting from the overall hull girder bending moment.

The description of the behavior of stiffened plates under predominantly compressive loads is relatively complicated, due to the large number of possible combinations of plate and stiffener geometry, boundary conditions and loading. It is possible to carry out accurate predictions of collapse load for any type of stiffened plate configuration, using one of the finite element formulations available.

The advantages of Y-stiffener plate combination are mentioned in [7].

The Y-stiffener has thirteen dimensions, eight of them can be calculated as a function of the other five dimension; namely h_w, t_f, t_w, b_p and L, which were selected to be the independent variables.

As shown in Fig. 1, the eight dependent variables are: h_h, b_f, b_{fh}, t_{fh}, t_{iw}, b_e, b_{iw} and t_p.

The independent variables that would be used for optimizing the Y-section are:

1. Thickness of the web t_w of the T-part of Y-stiffened panel.
2. Height of the web h_w of the T-part of Y-stiffened panel.

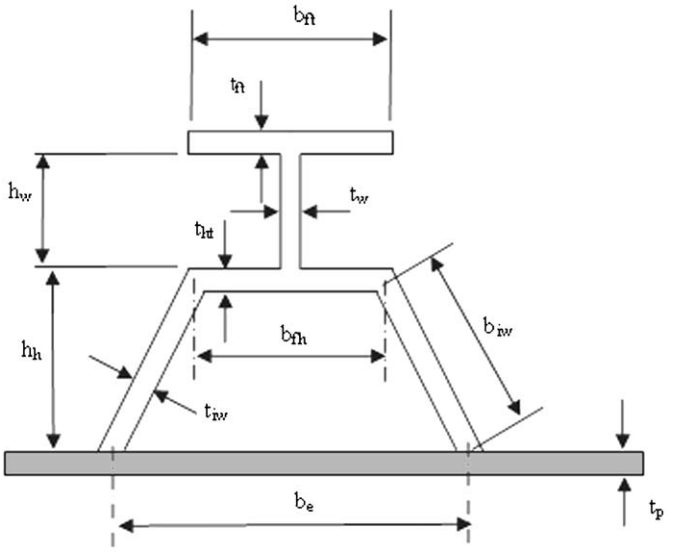

Fig. 1. Single Y-stiffener plate combination with five independent variables and dependent variables.

Table 1
Values of the five independent design variables.

Independent design variables (mm)				
t_w	h_w	b_p	t_f	L
15.1	431.2	1960	20.2	13,000
10.9	213.9	2240	10.9	18,000
7	145.5	2520	7	23,000

3. Breadth of the plate b_p.
4. Thickness of the flange t_f of the web of the T-part of Y-stiffened panel.
5. Increase in the length L of the Y-stiffened panel.

The independent variables are shown in Fig. 1 (see also Table 1)).

2. Finite element simulation

Finite element method technique, is employed to trace a full range of elastic–plastic behavior of the stiffened plates. To perform finite element analyses, the software had to offer combined geometrical and material nonlinear capabilities. In this study, the commercially available finite element code, ANSYS [13] was utilized.

Three possible values were selected for each of the five independent design variables. By combining the possible selected values of the five independent design variable, 3^5 variables combinations were generated. The analysis in this paper is made for each of these instances of variables.

2.1. Shell element formulation

The collapse load of the stiffened plates is calculated using the finite element software ANSYS by discretely stiffened plate approach. The four-node finite strain shell element (shell element 181) is used in this study. Geometric and material nonlinearity are considered in the analysis. The imperfections in the plate and the stiffener are not included in the finite element model. Simply supported boundary conditions are imposed on all the four edges of the plate, so as to simulate the test boundary conditions. The axial load is applied as uniform displacement at the nodes of the loaded edges.

2.2. Four-node finite strain shell element description

The four-node finite strain shell element is suitable for analyzing thin to moderately thick shell structures. It is a four-node element with six degrees of freedom at each node: translations in the x, y and z directions, and rotations about the x, y and z-axes. It is capable of representing plasticity, large displacement and large strain effects while accounting for changes in element thickness. The material constitutive behavior was defined as an elasto–plastic material with a von Mises yield criterion and a multilinear strain hardening rule. The four-node finite strain shell element is well-suited for linear, large rotation and/or large strain nonlinear applications. Change in shell thickness is accounted for in nonlinear analyses. In the element domain, both full and reduced integration schemes are supported. The four-node finite strain shell element accounts for follower (load stiffness) effects of distributed pressures, see Fig. 2.

To find a suitable choice of mesh divisions number, a convergence study was applied in which, a large number of mesh

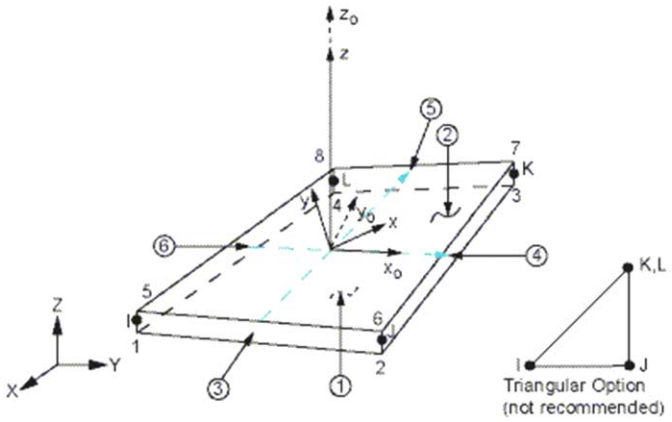

Fig. 2. The four-node finite strain shell element.

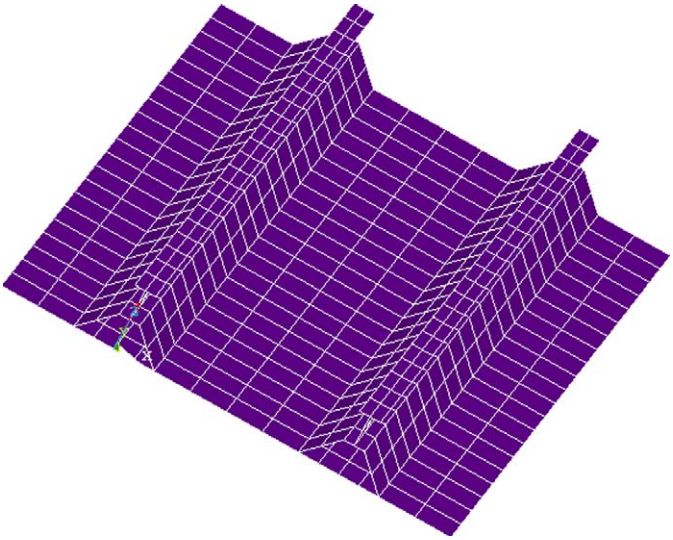

Fig. 3. Finite element mesh of Y-stiffened panel.

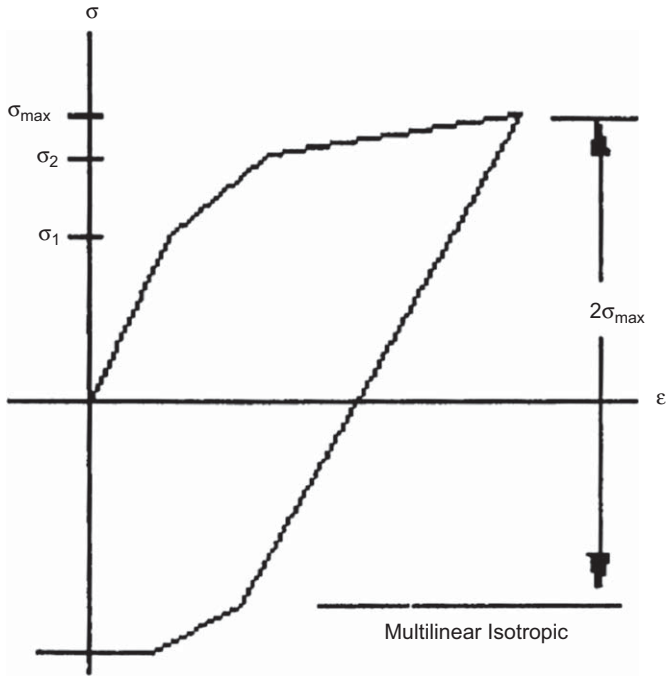

Fig. 4. Stress–strain behavior.

divisions was used and the ultimate buckling load is calculated, then the number of mesh divisions is reduced and the ultimate buckling load is calculated if the ultimate buckling load is approximately the same, then the number of mesh divisions is reduced once more, and so on until lowest number of mesh divisions which gives approximately the buckling load as the largest mesh divisions number is reached as shown in Fig. 3 and stress–strain behavior as shown in Fig. 4.

2.3. Boundary conditions for simply supported under longitudinal compression

Let a "0" on T[*x*, *y*, *z*] indicate translation constraints and on R[*x*, *y*, *z*] indicate rotational constraints about the *x*-, *y*- and *z*-coordinates. Let a "1" indicate no constraint.

All the plate nodes and stiffener nodes have equal *y*-displacements.

- The longitudinal edges are simply supported with T[1 1 0] and R[1 0 0], with all the nodes along each edge having equal *y*-displacement.
- The transverse edge on the upper edges, which is midlength of the mid-bay of the full double span–one bay model, has symmetric boundary conditions. This is simulated with T[0 1 1] and R[1 0 1].
- The transverse edge on the lower edges, which is the loaded edge, is simply supported with T[1 1 0] and R[0 1 0]. Only the plate nodes have equal *x*-displacements.
- The transverse cross-frame is not modeled, but is simulated with T[1 1 0]. Y-stiffener plate combination have 11 dimensions as basic dimensions as shown in Fig. 5, we selected five design variables as independent variables.

Three possible values were selected for each of the design variables. By combining the possible selected values of the design variable, 3^5 variables combinations were generated. For each of the 3^5 variable combinations, FEA was carried out to obtain an ultimate buckling strength.

2.4. Method of loading

The displacement control method was used for the analysis of the y-stiffened panel. Axial compressive load was applied to the Y-stiffened panel by specifying a displacement to the nodes at the front face and the back face is fixed of the Y-stiffened panel. Generally, different displacements were specified, and the displacement is equivalent to the axial shortening of the y-stiffened panel, see Fig. 6.

3. The effect of independent variables on the ultimate buckling load for Y-stiffener plate combination

The effect of the independent variables on the values of the ultimate buckling load and the weight which is related to the volume per unit area by multiplying it by the area and the density ($\rho b_p L$) must be known. The choice of the weight instead of the volume per unit area was basically to see the effect of L and b_p on the weight which cannot be seen if the volume per unit area is used as the horizontal axis.

Fig. 7(a and b) shows the increase in the thickness of the web t_w and the height of the web h_w leads to a tremendous increase in the maximum buckling load and to a slight increase in the weight of the Y-stiffened panels.

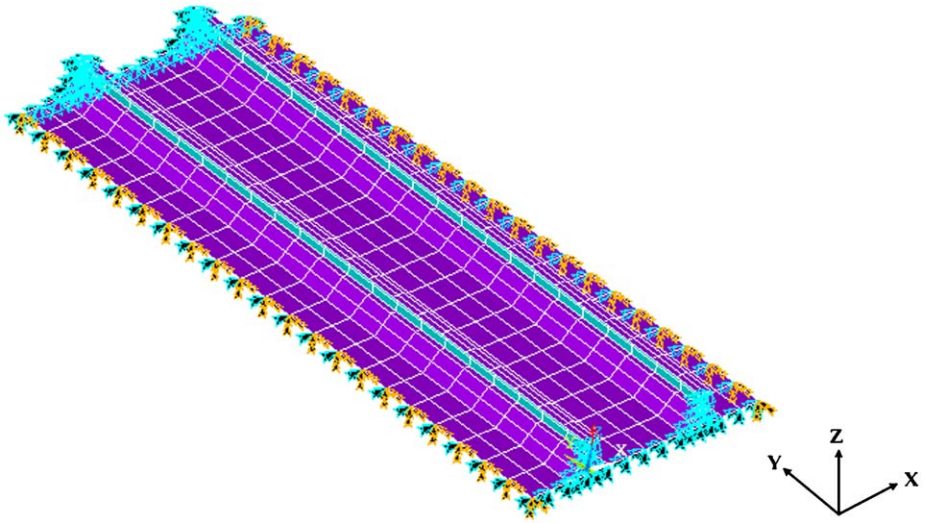

Fig. 5. Finite element boundary conditions of Y-stiffened panel.

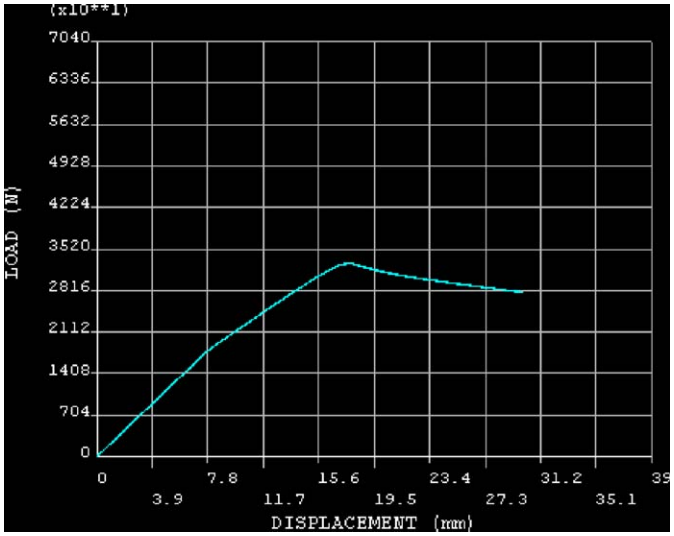

Fig. 6. Load versus displacement.

Fig. 7(c) shows the increase in the breadth of the plate b_p, leads to a slow increase in the maximum buckling load and to a significant increase in the weight of Y-stiffened panels.

Fig. 7(d) shows the increase in the thickness of the flange of the web t_f almost has no effect on the maximum load values; of course the weight of the Y-stiffened panels will increase.

Fig. 7(e) shows the increase in the length L of the Y-stiffened panel leads to a decrease in the maximum buckling load and to an increase in the weight of the Y-stiffened panels.

4. Surrogate function to calculate the ultimate buckling load for Y-stiffened panels

Finite element method should more be applied in the near future to direct quantitative estimation of the crashworthiness. Finite element analysis is considered to be numerical experiments at reasonable cost and also as an alternative to physical experiments. Finite element method is one of the most powerful approaches to analyze nonlinear behaviors of structures, but in usual it requires enormous computational efforts which are generally caused by a large number of unknowns and also complicated numerical integration, especially for obtaining the elastic–plastic stiffness matrix of the element. In other words, it takes a very long time to 243 cases. So, we suggested a new formulation is more than 1458 times faster than nonlinear finite element analyses. Where the crashworthiness of the hull structure deeply depends on the nonlinear elasto–plastic structural.

The polynomial used is a second degree polynomial that minimizes the residual function:

$$RSS = \sum_{i=1}^{n} (F_i^* - F(\mathbf{x}_i, \mathbf{C}))^2, \tag{1}$$

where n is the number of simulations; $\mathbf{x}_i$ is the set of values of the independent variables for which the finite element analysis is simulated; F^*_i is the ith maximum buckling load calculated using the finite element analysis corresponding to the sampling point $\mathbf{x}_i$; F is the surrogate function; $\mathbf{C}$ is the parameter of the surrogate function.

Table 4 shows the divisions of the independent variables. The divisions lead to 243 combinations of instances of the independent variables. Half of these combinations (122 instances) are used to fit the second-degree polynomial with a modification that involves the relaxation of the nonlinear shape of the maximum into a linear by taking the log of the approximated function. The rest of the combinations are used to test the fitting processes as shown in the latter sections. These values are used to make formulate the surrogate function as follows:

$$\log_e(\mathbf{F}^*) = \mathbf{X}^T\mathbf{A}\mathbf{X} + \mathbf{X}^T\mathbf{B} + \mathbf{C}', \tag{2}$$

where

$$\mathbf{X} = \begin{bmatrix} L \\ t_f \\ t_w \\ h_w \\ b_p \end{bmatrix}, \quad \mathbf{A} = \begin{bmatrix} c_1 & 0 & 0 & 0 & 0 \\ c_6 & c_2 & 0 & 0 & 0 \\ c_7 & c_{10} & c_3 & 0 & 0 \\ c_8 & c_{11} & c_{13} & c_4 & 0 \\ c_9 & c_{12} & c_{14} & c_{15} & c_5 \end{bmatrix}, \quad \mathbf{B} = \begin{bmatrix} c_{16} \\ c_{17} \\ c_{18} \\ c_{19} \\ c_{20} \end{bmatrix},$$

and $\mathbf{C}' = c_{21}$.

The expansion form of the approximate equation (2) can be written as follows:

$$\begin{aligned} \log_e F = {} & c_1L^2 + c_2t_f^2 + c_3t_w^2 + c_4h_w^2 + c_5b_p^2 + c_6Lt_f + c_7Lt_w + c_8Lh_w + c_9Lb_p \\ & + c_{10}t_ft_w + c_{11}t_fh_w + c_{12}t_fb_p + c_{13}t_wh_w + c_{14}t_wb_p + c_{15}h_wb_p \\ & + c_{16}L + c_{17}t_f + c_{18}t_w + c_{19}h_w + c_{20}b_p + c_{21}. \end{aligned} \tag{3}$$

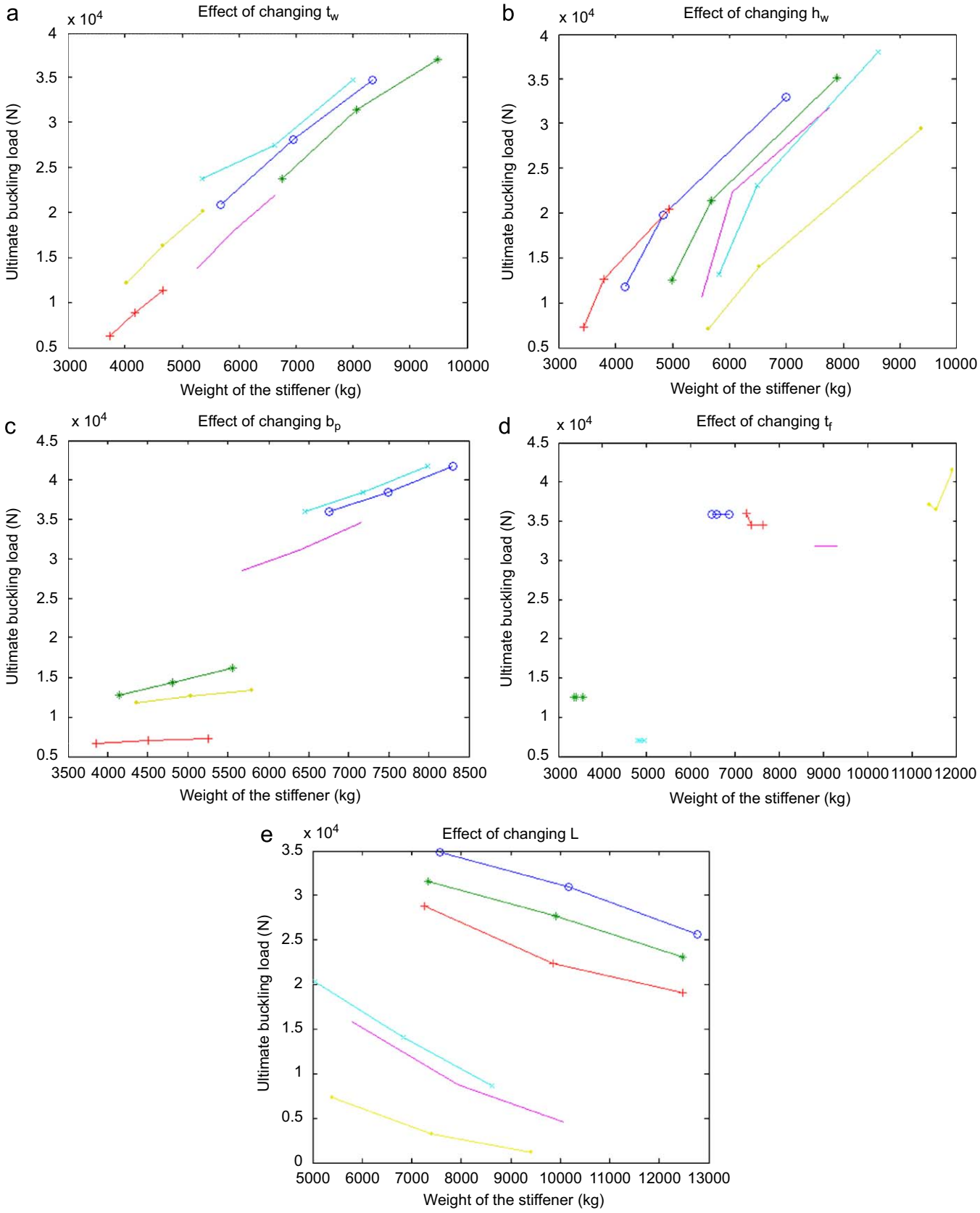

Fig. 7. Relation between the load and the weight for different sets of the other design variables (a) with changing t_w from 7 to 10.9 to 15.1 mm, (b) with changing h_w from 145.5 to 213.9 to 431.2 mm, (c) with changing b_p from 1960 to 2240 to 2520 mm, (d) with changing t_f from 7 to 10.7 to 20.2 mm and (e) with changing L from 13,000 to 18,000 to 23,000 mm.

$F = e^{\log(F)}$.

The 21 coefficients are evaluated using the pseudo-inverse notion which minimizes the least squares function (1)

$$\mathbf{C} = \begin{bmatrix} c_1 \\ c_2 \\ c_3 \\ \vdots \\ c_{21} \end{bmatrix} = \mathbf{D}^{-L}\log_e(\mathbf{F}^*),$$

where

$$\mathbf{D} = \begin{pmatrix} L_1^2 & t_{f_1}^2 & t_{w_1}^2 & h_{w_1}^2 & b_{p_1}^2 & L_1 t_{f_1} & \dots & 1 \\ L_2^2 & t_{f_2}^2 & t_{w_2}^2 & h_{w_2}^2 & b_{p_2}^2 & L_1 t_{f_2} & \dots & 1 \\ \vdots & \vdots & \vdots & \vdots & \vdots & \vdots & \dots & \vdots \\ \vdots & \vdots & \vdots & \vdots & \vdots & \vdots & \dots & \vdots \\ L_m^2 & t_{f_m}^2 & t_{w_m}^2 & h_{w_m}^2 & b_{p_m}^2 & L_1 t_{f_m} & \dots & 1 \end{pmatrix},$$

$\mathbf{D}^{-L} = (\mathbf{D}^T\mathbf{D})^{-1}\mathbf{D}^T$ is the pseudo-left inverse of the matrix $\mathbf{D}$, which will generate a least squares fit of the approximate function.

Table 2
The surrogate function coefficients.

c_1	−0.00000000246570	c_8	0.00000040477916	c_{15}	0.00000104971216
c_2	0.00095595541032	c_9	−0.00000002121483	c_{16}	−0.00010153533588
c_3	−0.00495326555890	c_{10}	0.00000668618988	c_{17}	−0.01898843779226
c_4	−0.00003152740100	c_{11}	0.00000530783008	c_{18}	0.18785755303179
c_5	−0.00000020275091	c_{12}	−0.00000348538704	c_{19}	0.01593280870991
c_6	−0.00000005614830	c_{13}	−0.00011623568028	c_{20}	0.00143271225138
c_7	0.00000309776708	c_{14}	−0.00001324434465	c_{21}	5.34693211464156

5. Validation of the surrogate function

The approximate maximum load equation has been tested with 121 instances of the design variables and the results were compared to the results of finite element analysis. The error was calculated according to

$$\text{Error} = \frac{F^* - F(\mathbf{x}, \mathbf{C})}{F^*}, \tag{4}$$

where F^* and $F(\mathbf{x}, \mathbf{C})$ are as defined in Eq. (1).

The error values were plotted using normal distribution plot as in Fig. 7, and it is almost a Gaussian distribution with zero mean, 0.0694 standard deviation. From the figure, it can be seen that the error will be within $\pm 15\%$ with probability 0.98. The twenty-one coefficients are listed in Table 2.

Fig. 8 depicts the statistical evaluation of the surrogate function. Table 3 gives a list of the approximate ultimate buckling load calculated using the surrogate function and the actual ultimate buckling load calculated, using finite element analysis for the 121 instances of the design variables which were used to test the surrogate function to be able to get the individual error of each set of the design variables.

6. The weight objective function

Weight minimization is an important objective in ship building. Not only that it affects the buoyancy of the boat, but in addition it contributes to the ship cost. Each stiffener adds to the overall weight of the ship in three forms. These are explained with the aid of Fig. 9.

The larger the cross-sectional area of the stiffener, the more weight is added to the ship total weight. In addition, the short stiffeners lead to better buckling strength, but this would mean more transverse girders to be added to the overall weight.

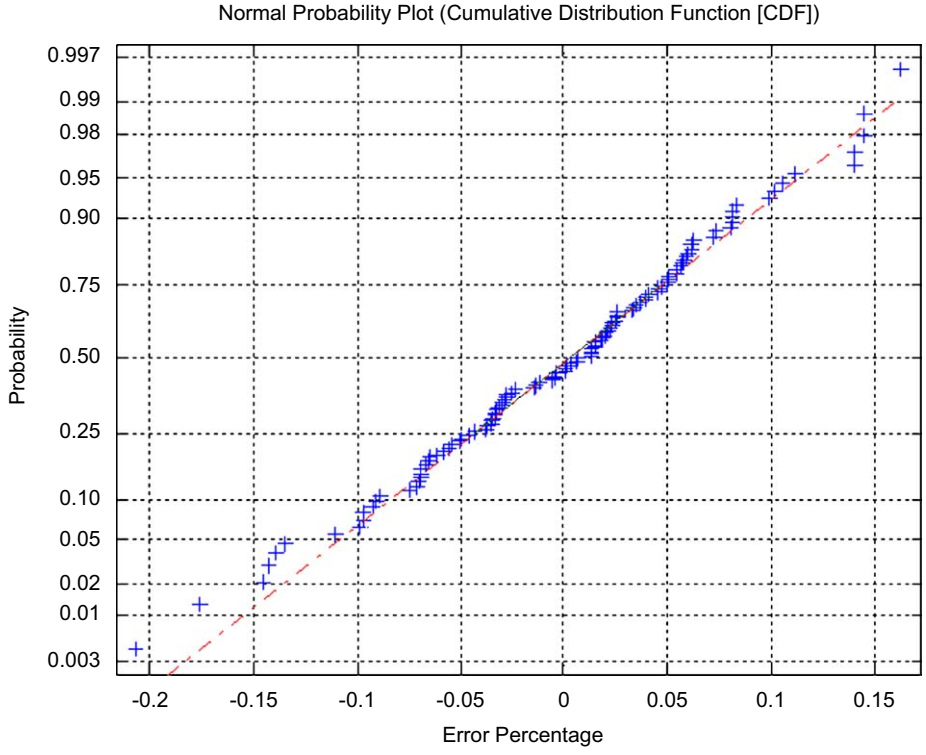

Fig. 8. A normal probability plot of the error of the surrogate function.

Table 3
A list of the approximate ultimate buckling load (UBS) calculated using the surrogate function (SF) and the actual ultimate buckling load calculated using the finite element analysis (FEA) for the 121 instances of the design variables which were used to test the surrogate function.

Y-model no.	UBS, SF	UBS, FEA	Y-model no.	UBS, SF	UBS, FEA	Y-model no.	UBS, SF	UBS, FEA
Y2	2.7824	2.8252	Y84	1.9219	2.0442	Y162	0.3424	0.3215
Y4	2.3314	2.036	Y86	1.1508	1.1098	Y164	2.1733	2.023
Y6	1.3443	1.2567	Y88	0.6497	0.6461	Y166	0.8606	0.862
Y8	0.9103	0.9238	Y90	0.3098	0.3277	Y168	0.3861	0.4511
Y10	3.5189	3.7075	Y92	2.956	2.7727	Y170	0.2237	0.2171
Y12	2.5655	2.3987	Y94	1.5727	1.5081	Y172	2.9498	2.7582
Y14	2.0758	1.8228	Y96	0.8243	0.8439	Y174	1.6734	1.7621
Y16	1.2169	1.2435	Y98	0.4987	0.5054	Y176	0.634	0.6842
Y18	0.678	0.7021	Y100	3.6937	4.0198	Y178	0.3209	0.3045
Y20	3.6537	3.3456	Y102	2.4479	2.2315	Y180	0.1391	0.1218
Y22	2.6117	2.3983	Y104	1.2532	1.2364	Y182	2.5341	2.4722
Y24	1.5992	1.5809	Y106	0.6588	0.6931	Y184	0.8561	0.9306
Y26	1.0106	1.0287	Y108	0.3336	0.3215	Y186	0.4079	0.4558
Y28	2.9148	3.4804	Y110	2.4905	2.6405	Y188	0.2205	0.2021
Y30	2.0633	2.3987	Y112	1.4497	1.4096	Y190	2.6066	2.6656
Y32	1.8245	1.6611	Y114	0.7377	0.8025	Y192	1.4357	1.5031
Y34	1.1119	1.1664	Y116	0.4635	0.4923	Y194	0.5944	0.6617
Y36	0.6014	0.6673	Y118	3.2919	3.2938	Y196	0.3128	0.3055
Y38	3.1049	3.0145	Y120	2.1182	2.0067	Y198	0.1317	0.1298
Y40	2.4282	2.2137	Y122	1.1851	1.1794	Y200	2.2972	2.2198
Y42	1.4435	1.4045	Y124	0.6476	0.6739	Y202	0.8491	0.8996
Y44	0.9472	0.9788	Y126	0.3184	0.3266	Y204	0.3928	0.4567
Y46	3.7781	4.0258	Y128	3.1383	3.0364	Y206	0.2205	0.2108
Y48	2.84	2.9754	Y130	1.5584	1.5785	Y208	3.0001	3.021
Y52	1.2184	1.3126	Y132	0.8421	0.8778	Y210	1.7547	1.9086
Y54	0.6999	0.7282	Y134	0.4938	0.5111	Y212	0.6212	0.6993
Y56	2.7166	2.7689	Y136	3.0167	3.0963	Y216	0.136	0.1127
Y58	2.3103	2.036	Y138	1.884	1.9542	Y218	2.1377	2.1812
Y60	1.3331	1.2567	Y140	1.145	1.1098	Y220	0.8592	0.862
Y62	0.9067	0.9238	Y142	0.6493	0.6461	Y222	0.3857	0.4511
Y64	3.4789	3.7075	Y144	0.3099	0.3277	Y224	0.2245	0.2171
Y66	2.5382	2.3987	Y146	2.9343	2.8427	Y226	2.938	2.7563
Y70	1.2274	1.2435	Y148	1.5845	1.5081	Y228	1.6679	1.6892
Y72	0.6843	0.7021	Y150	0.8311	0.8439	Y230	0.6414	0.6842
Y74	3.6604	3.4866	Y152	0.5051	0.5054	Y232	0.3261	0.3045
Y76	2.6556	2.3923	Y154	3.7128	3.5899	Y234	0.1415	0.1323
Y78	1.6272	1.5809	Y156	2.4623	2.52	Y236	2.5576	2.1751
Y80	1.0329	1.0287	Y158	1.2795	1.2364	Y238	0.877	0.9306
Y82	3.0795	3.0963	Y160	0.6756	0.6931	Y240	0.4181	0.4558

The values of ultimate buckling load are multiplied by 10^4.
The used unit is Newton.

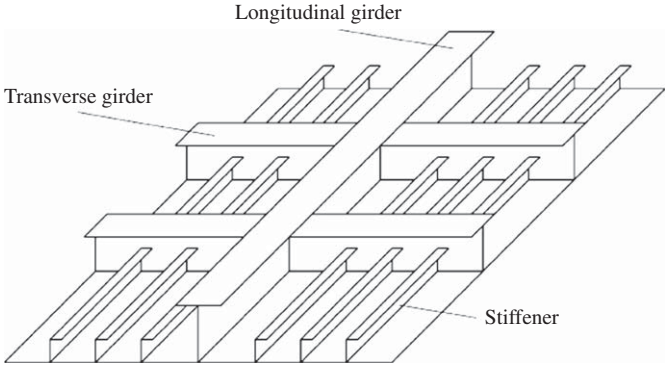

Fig. 9. Stiffened panel.

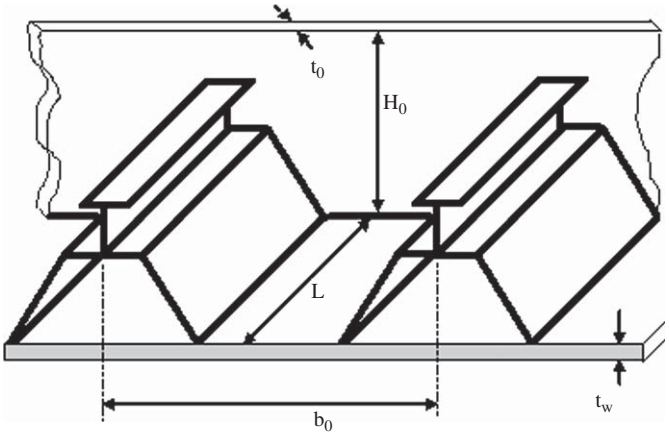

Fig. 10. A pair of stiffeners with a transverse girder at their end.

Likewise, a shorter distance between stiffeners leads to better panel strength, but that also leads to the addition of more stiffeners across the ship's breadth leading to extra weight. These factors should be reflected by the weight-objective functions.

Therefore, an equivalent weight objective function is devised to account for the above contributions. Fig. 10 shows a pair of stiffeners with a transverse girder at their end. Since the density is constant, then weight minimization is reflected by minimizing the volume contributed by the placement of a stiffener. The total volume contributed by a stiffener is equal to

$$V_{total} = V_{Stiffener} + V_{Plate} + V_{Girder},$$

where

1. The volume of the stiffener is given by its cross-sectional area multiplied by its length

$$V_{Stiffener} = A_{Stiffener} \times L.$$

2. The contribution of the stiffener to the volume of the plate beneath it is equal to the panel thickness multiplied by its length and the distance between two stiffeners.

$$V_{Plate} = b_p \times t_p \times L.$$

3. The contribution of the stiffener to the volume of the transverse girder is equal to the volume of the portion of the girder on which the stiffener is supported which is equal to

$$V_{Girder} = b_p \times t_G \times H_G.$$

where t_G is equal to the 1.5 × the web of the T-part thickness (t_w); H_G is equal to 2.5 × the total height of the stiffener.

The choice of the t_G and H_G were based on the standard values used in ship building.

In order to let the total volume function account for the placement of extra transverse girders when the stiffener is shorter as well as to account for the placement of extra stiffeners when the distance between stiffeners is shorter, the total volume is divided by the product of the stiffener's length and the distance between stiffeners. Hence, the equivalent weight used in optimizing the weight contribution of the stiffener is in effect a volume per unit area function and is equal to

$$W_{eq} = \frac{V_{total}}{b_p L}. \tag{5}$$

7. The problem statement

Given a set of design variables describing the geometry of the stiffened panel

$$\mathbf{x} = \{L,\ t_f,\ t_w,\ h_w,\ b_p\}.$$

Minimize the weight function $W_{eq}(\mathbf{x})$ and maximize the surrogate buckling strength function $F(\mathbf{x})$ which were defined in the previous sections, subject to

$$\begin{aligned} &13,000 \leqslant L \leqslant 23,000\\ &7 \leqslant t_w \leqslant 20\\ &7 \leqslant t_f \leqslant 15\\ &145.5 \leqslant h_w \leqslant 431\\ &1960 \leqslant b_p \leqslant 2520. \end{aligned} \tag{6}$$

It has be mentioned that the choice of the range of L was according to the standards of the length between two bulkheads, and t_f, t_w, h_w ranges was based on the standard T-stiffener dimensions in shipbuilding and the last independent variable b_p was based on the spacing between the two inclined webs of the hat-part of the Y-stiffener.

8. Results of optimization of the Y-stiffened panel with the strength Pareto optimization algorithm

The strength Pareto algorithm is run for the problem at hand with the following specifications:

1. Population size = 100.
2. Number of generations = 100.
3. Percentage of population subjected to the genetic operators per generation = 40%.

The outcome of the optimization search is shown in the Pareto front, displayed in Fig. 11. The front is composed of 100 points. However, some points are not on the front. Usually these points are the ones placed by boundary mutations looking for near bounds optima and, therefore, they should be discarded. Note that some points favor the equivalent weight function, while others favor the maximum buckling strength function. The middle points are the ones which tend to favor the maximization of the strength to weight ratio.

Table 4 presents the values of the design variables associated with each point on the Pareto front as well as the objective function values and the ratio between the maximum buckling load and the volume per unit area of the stiffener. A close look at the table shows that the first two independent variables always stayed at their lower bounds, while the other variables varied within their lower and upper bounds. As for the first independent variable, the stiffener's length, the shorter it is the higher the buckling strength of the stiffener. It is obvious that the buckling strength dominated this variable. However, conclusions should not be drawn hastily as the bounds presented can change from one ship application to another. Another close look at the table reveals that larger dimensions are associated with the last points in the table which correspond to the high values of the maximum buckling load function. It is obvious that higher strength goes hand in hand with the larger dimensions. It is also worth noting that the highest strength to volume per unit area ratio is obtained at points 87–90 which are on the high strength side. Therefore, using such ratio as a sole objective function might not necessarily yield good designs if the weight is more of importance.

The row at the table top corresponds to the lowest point on the Pareto front having the lowest volume per unit areas. The consecutive rows correspond to the locations on the front with monotonically increasing volumes per unit areas and maximum buckling loads. Note that for the last independent variable, which is the distance apart between the two stiffeners, high values of it are associated with the high stiffness solutions on the front. High stiffness meant that the larger dimensions (especially the height) are selected.

The maximum buckling load has been evaluated using the surrogate function described earlier. Since this function is an approximation to the actual function obtained using finite element analysis, it is useful to evaluate the percent error between the actual and the approximate functions at the important point

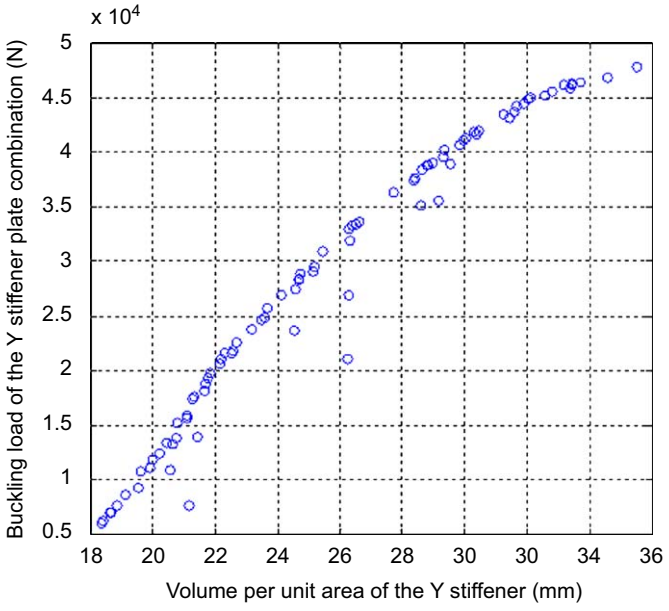

Fig. 11. The Pareto front of the optimization problem.

Table 4
The values of the design variables associated with each point on the Pareto front as well as the objective functions values and the ratio between the maximum buckling load and the volume per unit area of the stiffener.

Point number on Pareto front	Volume per unit area (mm)	Buckling load of Y-stiffener (N)	Maximum strength o Volume per unit area ratio (N/mm)	L (mm)	t_w (mm)	t_f (mm)	h_w (mm)	b_p (mm)
1	18.365	6051.7	329.53	13,268	7.0416	7	145.5	1978.6
2	18.388	6265.9	340.75	13,000	7	7	145.5	1978.6
3	18.62	6948.3	373.16	13,348	7.0003	7.1025	156.45	1960
4	18.676	6976.3	373.55	13,348	7.0003	7.1025	156.45	1970.1
5	18.86	7673.6	406.87	13,182	7	7	163.14	1977.6
6	19.108	8603.9	450.29	13,000	7.0006	7.2233	169.36	1960.1
7	19.551	9294.2	475.38	13,525	7	7.027	181.27	2015.6
8	19.601	10,777	549.82	13,000	7	7	191.93	1960
9	19.919	11,065	555.52	13,000	7	7	191.93	2020.8
10	19.99	11,912	595.91	13,255	7.0005	7.0754	203.43	1967.4
11	20.203	12,394	613.49	13,331	7	7.0001	207.76	1999.1
12	20.203	12,394	613.49	13,331	7	7.0001	207.76	1999.1
13	20.458	13,407	655.38	13,000	7	7.4516	209.27	1960
14	20.547	10,851	528.09	13,000	20.2	7	191.93	1960
15	20.619	13,257	642.94	13,296	7	7.4515	209.27	2001.7
16	20.619	13,257	642.94	13,296	7	7.4515	209.27	2001.7
17	20.757	13,776	663.68	13,000	7	7.4516	209.27	2020.8
18	20.78	15,256	734.2	13,547	7.005	7.004	236.19	1960
19	21.07	15,698	745.02	13,547	7.005	7.004	236.19	2020.8
20	21.089	15,865	752.26	13,515	7.0046	7.0063	237.35	2016.8
21	21.179	7665.5	361.93	23,000	7	7	273.83	2020.7
22	21.285	17,410	817.96	13,206	7.0004	7.028	248.31	1979.5
23	21.306	17,569	824.58	13,173	7	7.0303	249.47	1975.6
24	21.436	13,883	647.65	13,212	7	8.2457	201.13	2090.5
25	21.65	18,121	837	14,054	7.0011	7.0007	264.89	1992.9
26	21.713	18,754	863.75	13,643	7	7.0007	264.89	1992.9
27	21.772	19,320	887.39	13,280	7	7.0007	264.89	1992.9
28	21.839	19,798	906.55	13,000	7.0012	7.0191	264.93	1992.9
29	22.144	20,606	930.54	13,280	7	7	273.83	2020.7
30	22.193	21,054	948.71	13,000	7	7	273.83	2020.7
31	22.193	21,054	948.71	13,000	7	7	273.83	2020.7
32	22.289	21,561	967.36	13,093	7.0008	7.0278	285.77	1962.7
33	22.531	21,601	958.71	13,007	7	7.0918	270.06	2097.3
34	22.583	21,795	965.13	13,264	7	7.1978	278.07	2046.7
35	22.688	22,551	993.94	13,403	7	7	296.6	2006.2
36	23.178	23,803	1026.9	13,516	7	7	316.98	1993.2
37	23.178	23,803	1026.9	13,516	7	7	316.98	1993.2
38	23.473	24,677	1051.3	13,000	7	7	328.36	1960
39	23.599	24,855	1053.2	13,000	7.001	7.0006	332.75	1960
40	23.675	25,693	1085.3	13,178	7.0256	7	308.59	2147.6
41	23.675	25,693	1085.3	13,178	7.0256	7	308.59	2147.6
42	24.102	26,935	1117.5	13,000	7	7	328.36	2116.9
43	24.555	23,689	964.73	13,000	7	9.9637	241.85	2153.5
44	24.58	27,392	1114.4	13,609	7.214	7	339.48	2184
45	24.58	27,392	1114.4	13,609	7.214	7	339.48	2184
46	24.677	28,302	1146.9	13,052	7.0389	7	339.48	2184
47	24.685	28,394	1150.3	13,000	7	7	339.48	2184
48	24.685	28,394	1150.3	13,000	7	7	339.48	2184
49	24.685	28,394	1150.3	13,000	7	7	339.48	2184
50	24.726	28,893	1168.5	13,000	7	7	328.36	2258
51	25.143	29,098	1157.3	13,268	7	7.3788	340.83	2190.4
52	25.197	29,462	1169.3	13,030	7	7.3788	340.83	2190.4
53	25.452	30,896	1213.9	13,000	7	7	331.78	2393.4
54	26.254	21,071	802.58	13,547	7.005	7.004	431.2	1960
55	26.283	26,878	1022.7	16,912	7.235	7.6746	346.94	2479
56	26.284	32,991	1255.2	13,000	7	7.0068	339.96	2520
57	26.303	31,836	1210.3	13,052	7	8.4272	296	2462
58	26.38	33,248	1260.4	13,006	7	7.226	334.11	2520
59	26.522	33,417	1260	13,000	7	7	350.24	2520
60	26.623	33,629	1263.1	13,006	7	7.226	350.24	2488.5
61	27.734	36,295	1308.7	13,000	7	9.0548	331.78	2393.4
62	27.734	36,295	1308.7	13,000	7	9.0548	331.78	2393.4
63	28.378	37,419	1318.6	13,209	7	9.5168	336.48	2402.5
64	28.416	37,643	1324.7	13,341	7.0426	9.3522	334.11	2480
65	28.586	35,129	1228.9	13,000	7	12.136	278.44	2295.4
66	28.628	38,342	1339.3	13,209	7	9.5168	334.11	2480
67	28.79	38,763	1346.4	13,209	7	9.5168	336.48	2500.2
68	28.801	38,841	1348.6	13,172	7	9.5168	336.48	2500.2
69	28.985	38,975	1344.7	13,295	7.0368	9.82	335.19	2483.1
70	29.167	35,570	1219.5	13,000	7	10.561	350.24	2102.7
71	29.296	39,559	1350.3	13,000	7	9.4867	353.68	2483.3
72	29.355	40,206	1369.6	13,000	7	9.7992	342.02	2502.7

Table 4 (*continued*)

Point number on Pareto front	Volume per unit area (mm)	Buckling load of Y-stiffener (N)	Maximum strength o Volume per unit area ratio (N/mm)	L (mm)	t_w (mm)	t_f (mm)	h_w (mm)	b_p (mm)
73	29.534	38,915	1317.6	13,294	7	11.67	305.56	2400.7
74	29.836	40,652	1362.5	13,268	7.0416	10.387	342.02	2479.6
75	29.836	40,652	1362.5	13,268	7.0416	10.387	342.02	2479.6
76	29.836	40,652	1362.5	13,268	7.0416	10.387	342.02	2479.6
77	29.959	41,034	1369.7	13,016	7	10.363	346	2462.9
78	30.042	41,289	1374.4	13,018	7	10.447	344.72	2471.5
79	30.314	41,848	1380.5	13,000	7.0034	10.707	343.79	2472.3
80	30.383	41,663	1371.3	13,171	7	10.561	350.24	2488.9
81	30.442	41,985	1379.2	13,000	7	10.561	350.24	2488.9
82	31.247	43,477	1391.4	13,130	7.0193	11.592	341.35	2492.1
83	31.451	43,090	1370.1	13,000	7.0002	10.863	365.34	2520
84	31.573	43,684	1383.6	13,280	7	12.292	332.81	2477.9
85	31.678	44,256	1397	13,000	7	12.292	332.81	2477.9
86	31.903	44,377	1391	13,126	7.0399	12.38	336.81	2479.9
87	32.035	44,862	1400.4	13,046	7.0058	12.318	339.36	2499.6
88	32.099	44,933	1399.8	13,046	7.0058	12.318	340.94	2499.6
89	32.099	44,933	1399.8	13,046	7.0058	12.318	340.94	2499.6
90	32.099	44,933	1399.8	13,046	7.0058	12.318	340.94	2499.6
91	32.569	45,167	1386.8	13,317	7	12.786	342.02	2502.7
92	32.812	45,531	1387.6	13,324	7	12.916	343.55	2513.5
93	33.167	46,188	1392.6	13,046	7.0058	13.274	340.94	2499.6
94	33.373	45,821	1373	13,268	7.0416	13.552	342.02	2479.6
95	33.431	46,149	1380.4	13,052	7.0389	13.416	344.73	2479.5
96	33.449	46,263	1383.1	13,000	7	13.416	344.73	2479.5
97	33.704	46,378	1376.1	13,052	7.0389	13.416	350.24	2488.5
98	34.579	46,825	1354.1	13,000	7	15.1	328.36	2488.9
99	34.579	46,825	1354.1	13,000	7	15.1	328.36	2488.9
100	35.522	47,747	1344.1	13,000	7	15.092	346.57	2505.7

Table 5
The buckling load of the optimal dimensions of Y-stiffened panel, using FEA and the surrogate function and the error percentage between them.

	Buckling load of Y-stiffener (N)	L (mm)	t_w (mm)	t_f (mm)	h_w (mm)	b_p (mm)
Point 87 applied on FEA	21,424.5	13,046	7.0058	12.318	339.36	2499.6
Point 87 on the Pareto front (optimization)	22,431	13,046	7.0058	12.318	339.36	2499.6
Error percentage	4.7					

Table 6
A comparison between the results of single-objective optimization and multi-objective optimization (best Pareto front).

	Volume per unit area (mm)	Buckling load of Y-stiffener (N)	Maximum strength to volume per unit area ratio (N/mm)	L (mm)	t_w (mm)	t_f (mm)	h_w (mm)	b_p (mm)
Optimal point obtained by maximizing buckling strength to volume per area ratio	29.03	22,482	774.4	13,000	7	12.252	336.02	2520
Point 87 on the Pareto front	29.1204	22,431	770.28	13,046	7.0058	12.318	339.36	2499.6

(see Table 5). The point selected would be the one having the highest strength to volume per unit area ratio, i.e., point 87.

A common check that is used to test the obtained Pareto front does not need further iterations is to run a single objective optimization of an utility function and see if the outcome would lie on the Pareto front. This check is done by maximizing the ratio between the maximum buckling load and the volume per unit area. The method used for search is real-coded genetic algorithms. This single run yielded the results shown in Table 6, which by close observation appears to be almost identical with point 87 on the Pareto front.

9. Sensitivity analysis

The aim of the sensitivity analysis is to test and validate the result of the multi-objective optimization problem, which is the set of the optimum five design variables that gives the maximum strength to volume per unit area. For sensitivity analysis purposes 10,000 sets of design variables were randomly generated with uniform distribution in a range of $\pm 5\%$ around the optimum value of each design variable. The number 10,000 is the large sample size, normally used in Monte Carlo simulation [14]. For each of the 10,000 sets, the volume per unit area and the maximum buckling

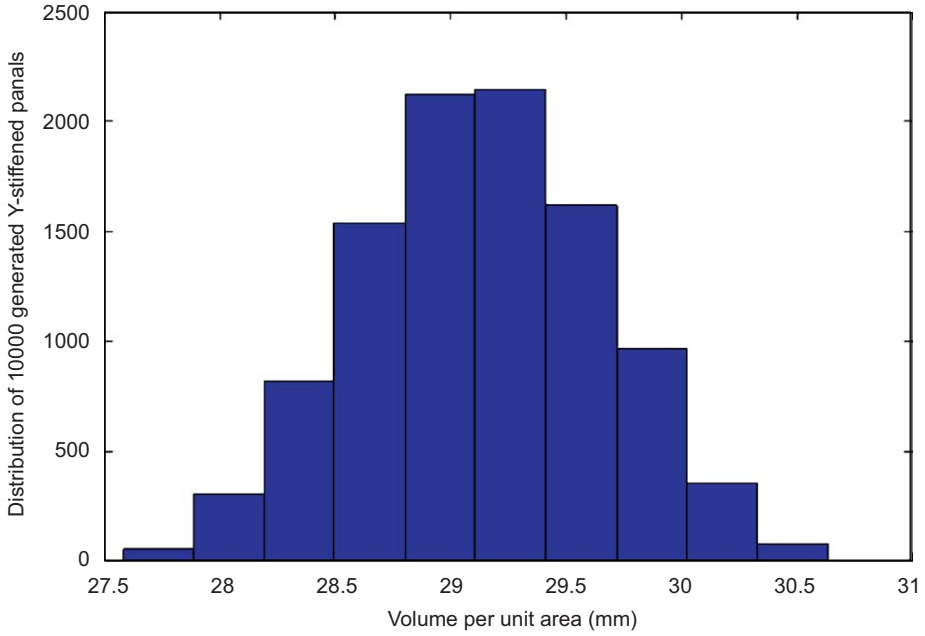

Fig. 12. Histogram of the volume per unit area of the 10,000 randomly generated sets of design variables.

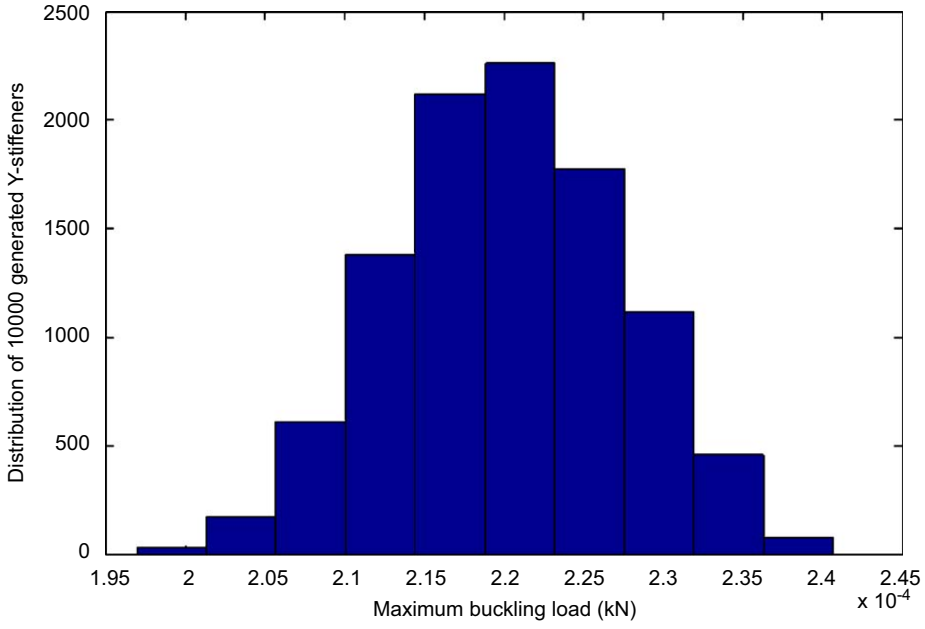

Fig. 13. Histogram of the maximum buckling load of the 10,000 randomly generated sets of design variable.

load were calculated and the mean and standard deviation were calculated for the 10,000 values of the two objective functions. It was found that the mean of the volume per unit area is 29.1324 mm and the mean of the maximum buckling load is 22,019.59 N. These values were compared to the volume per unit area and the maximum buckling load of the optimum set of design variables which are 29.1204 mm and 22,118.46 N, respectively, and the results were very close to the mean values calculated from the 10,000 randomly generated sets. Thus, the optimum set of design variables is validated using the sensitivity analysis procedure. Figs. 12 and 13 show the histogram of the 10,000 values of the two objective functions.

10. Conclusion

In this paper, the multi-objective optimization with real-coded genetic algorithm was used to design an optimum Y-stiffener plate combination. Five of the Y-stiffened panel dimensions were chosen to be the independent design variables of the optimization problem. The ultimate buckling load and the volume per unit area of the Y-stiffener plate combination are the objective functions. In order to calculate the ultimate buckling load of 243 different sets of the design variables with certain ranges for the design variables nonlinear finite element analysis was used. Using the values of the ultimate buckling loads calculated using nonlinear finite element

analysis, a new surrogate load function to predict the ultimate buckling load of Y-stiffener plate combination is created and validated. The proposed surrogate load function is validated only in certain ranges of the design variables. The effects of independent variables on the ultimate buckling load for Y-stiffener plate combination are carried out. Using multi-objective optimization with genetics algorithm, the Pareto optimal sets were calculated and the optimum set was selected as the set which has the maximum ultimate buckling load to volume per unit area ratio. Sensitivity analysis technique was used to test and validate the optimum set.

References

[1] Timoshenko SV, Gere JM. Theory of elastic stability. New York: McGraw-Hill; 1961.
[2] Bleich F. Buckling strength of metal structures. New York: McGraw-Hill Book Co.; 1952.
[3] Paik JK, Thayamballi AK. Ultimate limit state design of steel-plated structures. New York: Wiley; 2003.
[4] Paik JK, Thayamballi AK, Park YI. Local buckling of stiffeners in ship plating. Journal of Ship Research 1998;42(1):56–67.
[5] Ludolphy Hans. The unsinkable ship-development of the Y-shape support web, Royal Schelde Shipyard. The Netherlands Proceedings of the Second International Conference on Collision and Grounding of Ships, Copenhagen, Denmark, July 1–3, 2001.
[6] Badran Sherif Faruok, Nassef Ashraf O, Metwalli Sayed M. Stability of Y-stiffeners in ship plating under uniaxial compressive loads. Ships and Offshore Structures 2007;2(1):87–94.
[7] Badran Sherif Faruok, Nassef Ashraf O, Metwalli Sayed M. A comparison of buckling strength of Y- and T-stiffeners in ship plating Sname. Marine technology 2008;45(3):125–31.
[8] Klanac A, Ehlers S, Tabri K, Rudan S, Boekhuijsen J. Qualitative design assessment of crashworthy structures. Maritime transportation and exploitation of ocean and coastal resources. London: Taylor and Francis Group; 2005.
[9] Ghavami Khosrow, Mohammad Reza Khedmati. Numerical and experimental investigations on the compression behaviour of stiffened plates. Journal of Constructional Steel Research 2006;62(11):1087–100.
[10] Ben Young. Bifurcation analysis of thin-walled plain channel compression members. Finite Elements in Analysis and Design 2004;41(2):211–25.
[11] Kolakowski Z, Kubiak T. Load-carrying capacity of thin-walled composite structures. Composite Structures 2005;67(4):417–26.
[12] Yong Bai. Marine structural design. Amsterdam: Elsevier Science; 2003.
[13] Houston: Swanson Analysis Systems, Inc.; ANSYS Theory Manual and User Manual, ANSYS, Structural U, (version 10), 2005.
[14] James N. Siddall. Probabilistic engineering design-principles and applications. New York: Marcel Dekker; 1983.